Supporting Information for:

CO_2 hydrogenation to Higher alcohols over K-promoted bimetallic Fe-In catalysts on a Ce-ZrO_2 support

Xiaoying Xi [a,+], Feng Zeng [b,+], Heng Zhang [c], Xiaofeng Wu [d,e], Jie Ren [b], Timo Bisswanger [f], Christoph Stampfer [f], Jan P. Hofmann [d,e], Regina Palkovits [b,*], Hero J. Heeres [a,*]

[a] Green Chemical Reaction Engineering, Engineering and Technology Institute Groningen, University of Groningen, Nijenborgh 4, 9747 AG Groningen, The Netherlands

[b] Chair of Heterogeneous Catalysis and Chemical Technology, ITMC, RWTH Aachen University, Worringerweg 2, 52074 Aachen, Germany

[c] Zernike Institute for Advanced Materials, University of Groningen, Nijenborgh 4, 9747 AG, Groningen, the Netherlands

[d] Laboratory of Inorganic Materials and Catalysis, Department of Chemical Engineering and Chemistry, Eindhoven University of Technology, P.O. Box 513, 5600 MB Eindhoven, The Netherlands

[e] Surface Science Laboratory, Department of Materials and Earth Sciences, Technical University of Darmstadt, Otto-Berndt-Strasse 3, 64287 Darmstadt, Germany

[f] 2nd Institute of Physics A, RWTH Aachen University, 52074 Aachen, Germany

[+] These authors have contributed equally.

[*] Corresponding author: palkovits@itmc.rwth-aachen.de (Regina Palkovits), h.j.heeres@rug.nl (Hero J. Heeres).

Number of Pages: 29

Number of Figures: 18

Number of Tables: 8

Table S1. Catalyst synthesis: intakes of $In(NO_3)_3 \cdot xH_2O$ and $Fe(NO_3)_3 \cdot 9H_2O$ for the synthesis of the catalysts, and the theoretical In and Fe loadings in the prepared FeIn/Ce-ZrO_2 catalysts in weight percent.

Catalyst	Mass (g) of $In(NO_3)_3 \cdot xH_2O$	Mass (g) of $Fe(NO_3)_3 \cdot 9H_2O$	Weight percent loading (%) of In	Weight percent loading (%) of Fe
In/Ce-ZrO_2	1.52	0	9.09	0
0.18-FeIn/Ce-ZrO_2	1.22	0.32	7.93	0.86
0.48-FeIn/Ce-ZrO_2	0.76	0.80	4.61	2.07
0.82-FeIn/Ce-ZrO_2	0.30	1.28	1.70	3.69
0.88-FeIn/Ce-ZrO_2	0.15	1.44	1.05	3.84
Fe/Ce-ZrO_2	0	1.60	0	3.98

Table S2. Intakes of FeIn/Ce-ZrO_2 and K_2CO_3 for the preparation of the K-FeIn/Ce-ZrO_2 catalysts.

K content	Mass (g) of FeIn/Ce-ZrO_2	Mass (g) of K_2CO_3
1%	0.3929	0.0071
4%	0.3717	0.0283
7%	0.3505	0.0495

Evaluation of possible External Mass Transfer limitations

The absence of external mass transfer limitations was checked by estimating Mears criteria (eq.S1 [1]).

$$C_{Mears} = \frac{-r_{obs} \cdot \rho_b \cdot d_p \cdot n_A}{2.k_c \cdot C_b} \quad \text{(S1)}$$

where d_p is the diameter of catalyst pellets, n_A is the reaction order, and C_b is the gas concentration in bulk gas phase. The observed reaction rate can be determined from molar flow rate F_i, and the mass of the catalyst bed m_{cat}:

$$-r_{obs} = \frac{F_i}{m_{cat}} \quad \text{(S2)}$$

The density of the catalyst bed can be determined by:

$$\rho_b = \frac{m_{cat}}{V_{bed}} \quad \text{(S3)}$$

The mass transport coefficient (k_c) can then be calculated from the following equations:

$$k_c = \frac{Sh \cdot D_{ab}}{d_p} \quad \text{(S4)}$$

$$Sh = 2 + 0.6\, Re^{1/2}\, Sc^{1/3} \quad \text{(Frössling correlation, [2])} \quad \text{(S5)}$$

$$Re = \frac{v_0 . d_p}{\nu} \quad \text{(S6)}$$

$$v_0 = \frac{V_0}{A_{reactor}} \quad \text{(S7)}$$

where V_0 is the volumetric flow rate, ν is the kinetic viscosity and $A_{reactor}$ is the cross-sectional area of the tube reactor.

$$Sc = \frac{\nu}{D_{ab}} \quad \text{(S8)}$$

$$\nu = \frac{\mu}{\rho} \quad \text{(S9)}$$

$$\mu = 2.66.10^{-6}\frac{\sqrt{MT}}{\sigma^2\Omega} \quad \text{(S10)}$$

$$\Omega = \frac{1.16145}{(\frac{\kappa T}{\varepsilon})^{0.148}} + \frac{0.5248}{\exp(0.77.\frac{\kappa T}{\varepsilon})} + \frac{2.1617}{\exp(2.43.\frac{\kappa T}{\varepsilon})} \quad \text{(S11)}$$

$$D_{ab} = 0.0018583\sqrt{T^3(\frac{1}{M_a} + \frac{1}{M_b})}\frac{1}{P\,.\,\sigma^2\,.\Omega} \quad \text{(S12)}$$

[3]

where ρ is the density of reactant, σ is a characteristic collision diameter for the molecule [4], M is the molar mass of the molecule, T is the temperature, and $\frac{\kappa}{\varepsilon}$ is a parameter in the Lennard-Jones potential equation. [4]

The calculated value of C_{Mears} was 1.5×10^{-11} (« 0.15), which indicates the absence of external mass transfer limitations.

Internal Mass Transfer Evaluation

The Weisz-Prater criterion [5] was used to evaluate the absence of internal diffusion limitations (eq. S13).

$$C_{WP} = \frac{-r_{obs}\,.\,\rho_c\,.\,r^2}{D_e C_S} \quad \text{(S13)}$$

where ρ_c is the density of the catalyst and C_S is the reactant concentration at the surface of the catalyst. The external mass transport limitations were estimated to be negligible, so the reactant concentration at the surface of the catalyst is identical to the bulk concentration ($C_S = C_b$). D_e is the effective diffusion coefficient in the pores of the catalyst. The Knudsen correlation (D_K, [6]) could be used for the calculation of D_e.

$$D_e = 1.25\,D_k \quad \text{(S14)}$$

$$D_K = 0.097 * d_p(\frac{T}{M})^{0.5} \quad \text{(S15)}$$

The resulting value of the Weisz-Prater correlation is 3.6×10^{-4} (« 1), suggesting that the internal diffusion is not significant.

Table S3. Duplicate experiments showing CO_2 conversion and product selectivity for the K-0.82-FeIn/Ce-ZrO_2_900 catalyst (in the presence of SiC_900). [a]

Item	X_{CO_2} [b] (%)	Selectivity (%)						
		CH_4	C_{2-4} olefins[c]	C_{2-4} paraffins[d]	CO	Methanol	HA	Others[e]
Run 1	29.6	20.1	20.3	12.5	13.4	4.7	28.7	0.3
Run 2	28.7	21.3	20.5	12.8	14.2	4.2	26.7	0.3

[a] Reaction conditions: 300 °C, 10 MPa, GHSV = 4500 mL g^{-1} h^{-1}, H_2/CO_2 = 3; [b] CO_2 conversion; [c] Olefins with carbon number of 2 to 4; [d] Paraffins with carbon number of 2 to 4; [e] Other hydrocarbons and liquid oxygenates except alcohols.

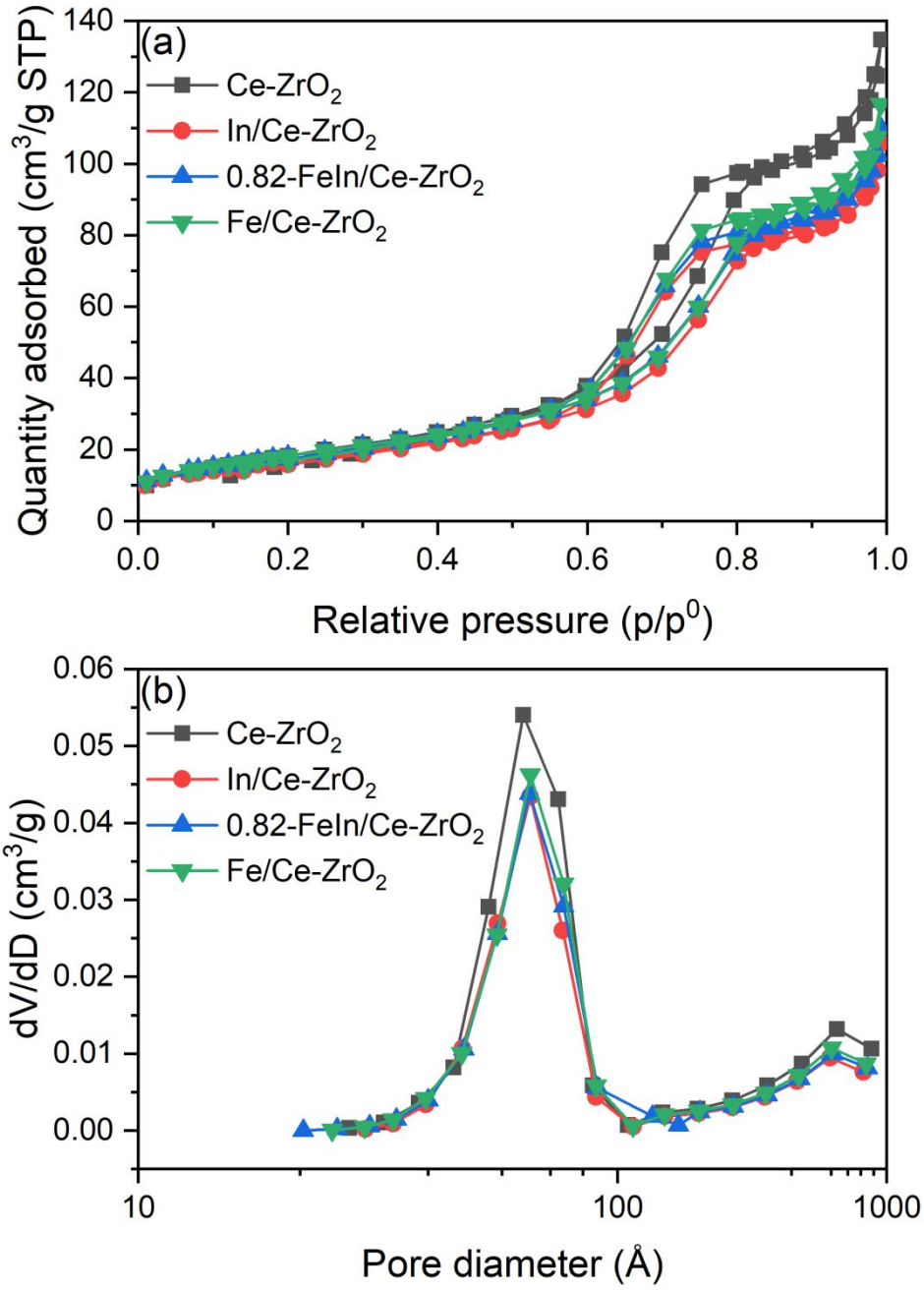

Figure S1. N_2 adsorption-desorption isotherms (a) and pore diameter distributions (b) of Ce-ZrO_2, In/Ce-ZrO_2, 0.82-FeIn/Ce-ZrO_2 and Fe/Ce-ZrO_2.

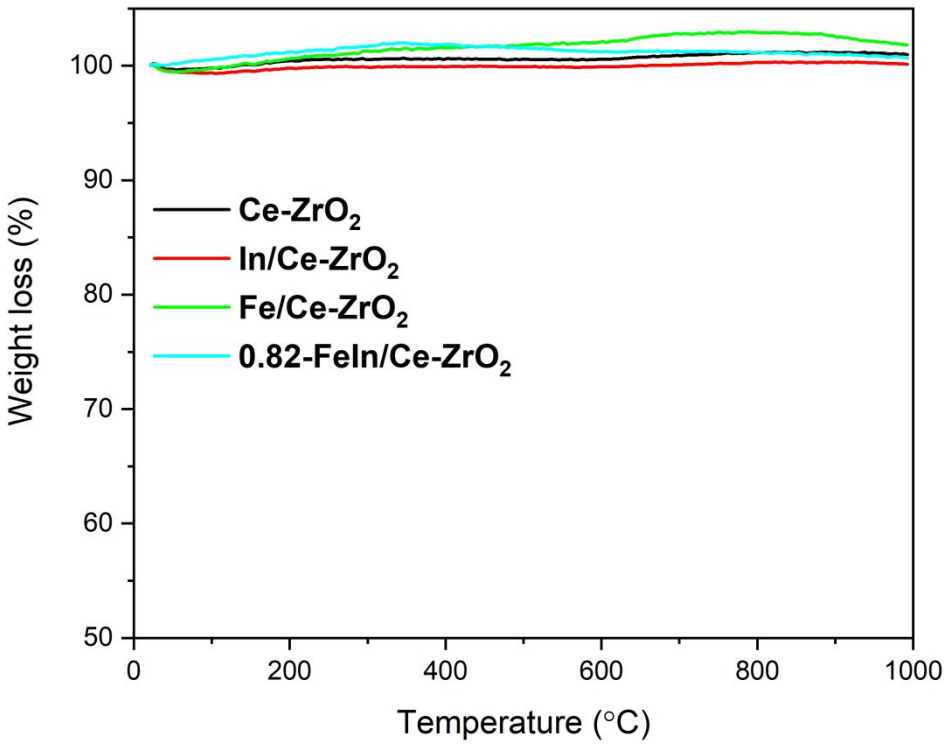

Figure S2. TGA profiles of Ce-ZrO_2, In/Ce-ZrO_2, 0.82-FeIn/Ce-ZrO_2 and Fe/Ce-ZrO_2 under N_2 atmosphere.

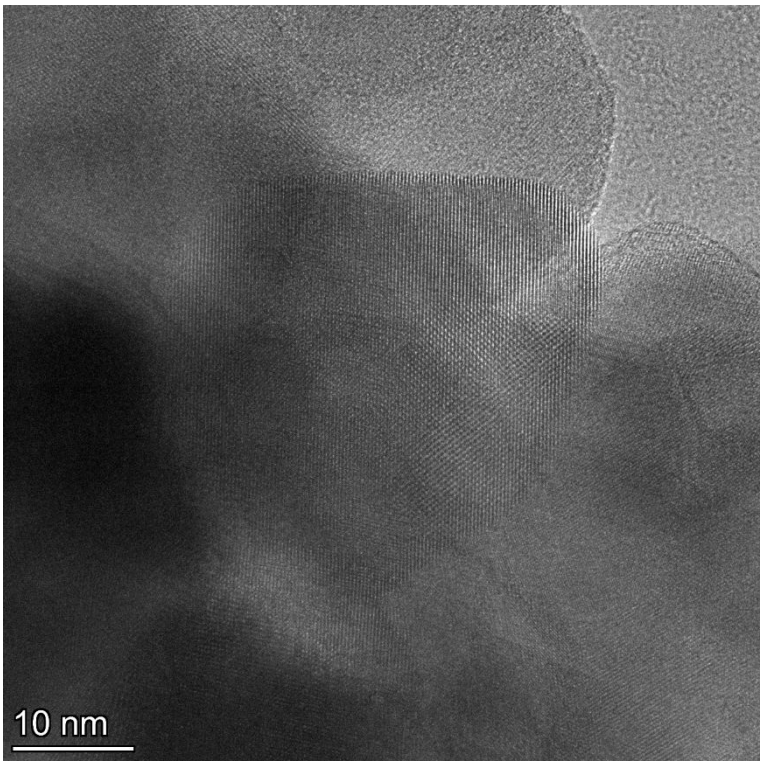

Figure S3. Typical TEM image of the 0.82-FeIn/Ce-ZrO_2 catalysts.

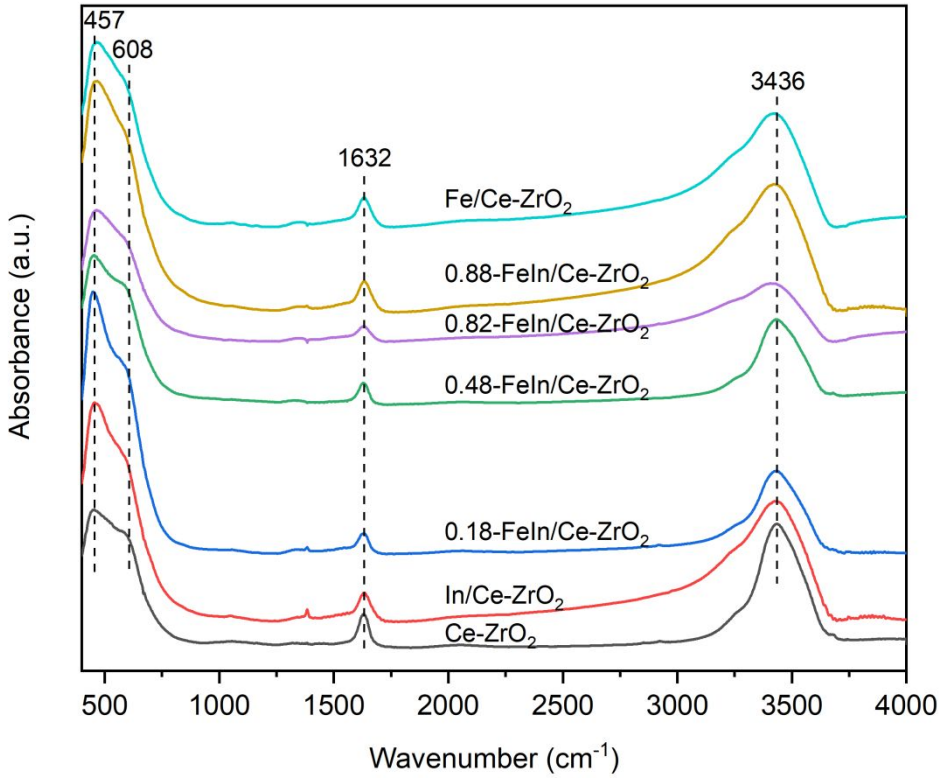

Figure S4. FTIR spectra of the Ce-ZrO_2 and FeIn/Ce-ZrO_2 catalysts with different Fe/(Fe+In) molar ratios.

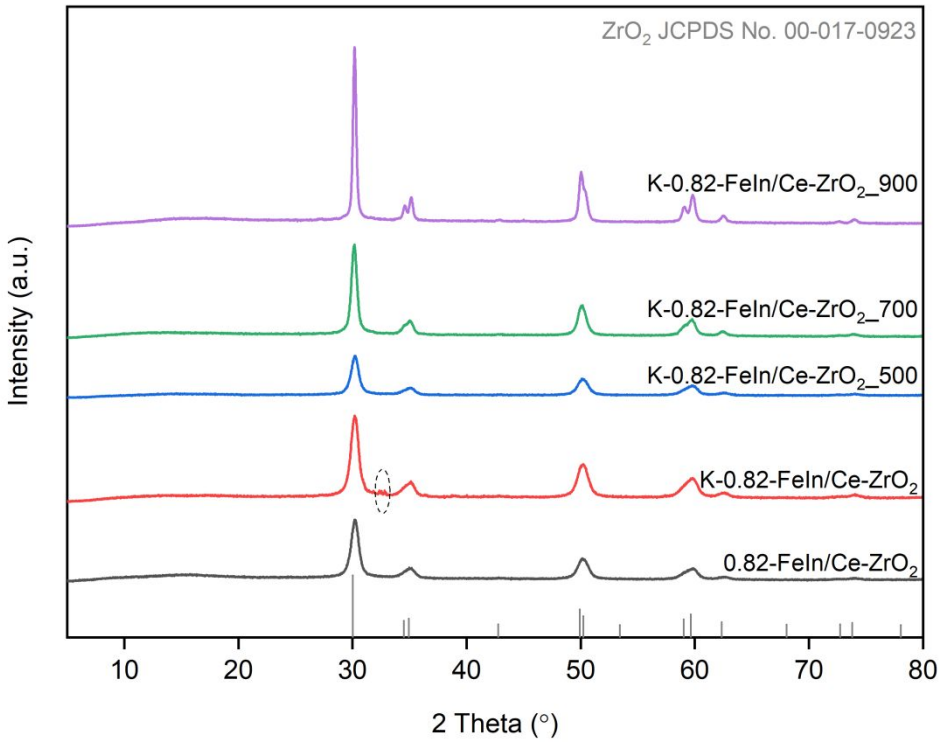

Figure S5. XRD patterns of 0.82-FeIn/Ce-ZrO_2 and K-0.82-FeIn/Ce-ZrO_2 catalysts after calcination at different temperature.

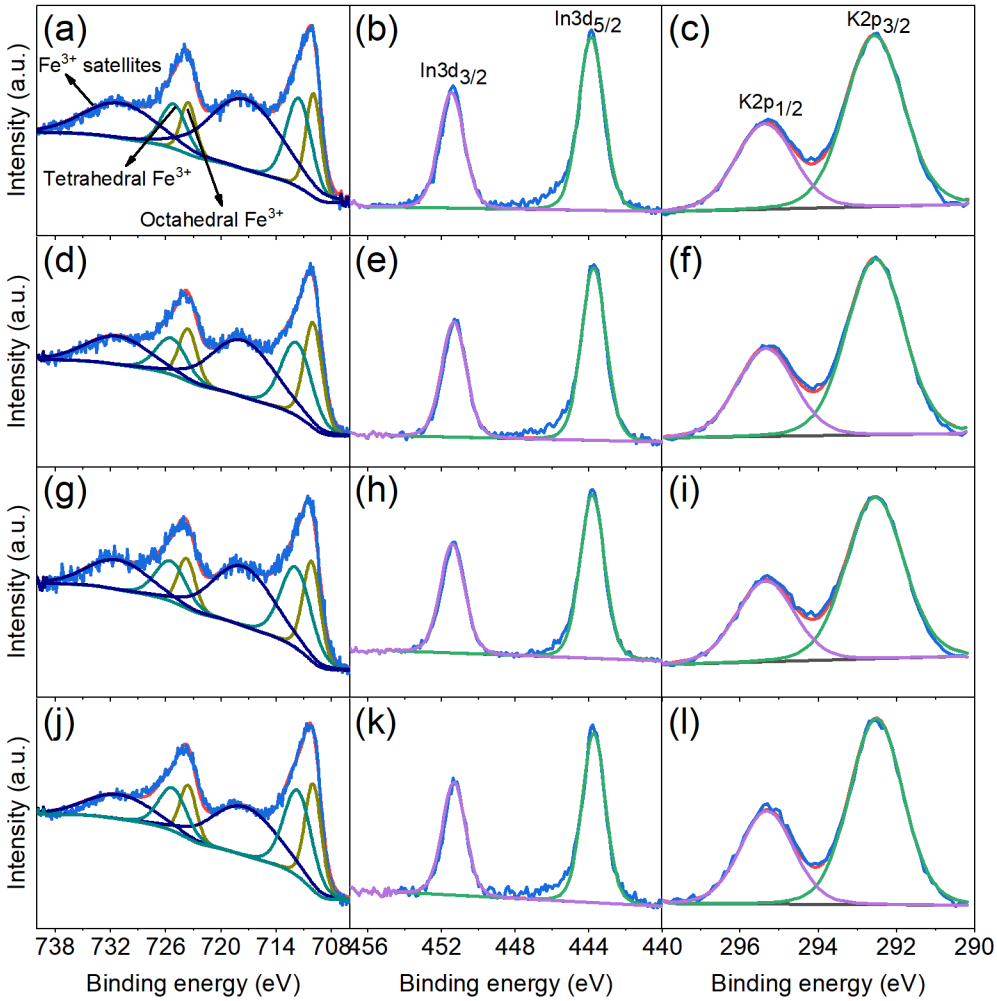

Figure S6. Deconvolutions of XPS spectra: Fe2p, In3d and K2p spectra of K-0.82-FeIn/Ce-ZrO_2 (a, b and c), K-0.82-FeIn/Ce-ZrO_2_500 (d, e and f), K-0.82-FeIn/Ce-ZrO_2_700 (g, h and i) and K-0.82-FeIn/Ce-ZrO_2_900 (j, k and l).

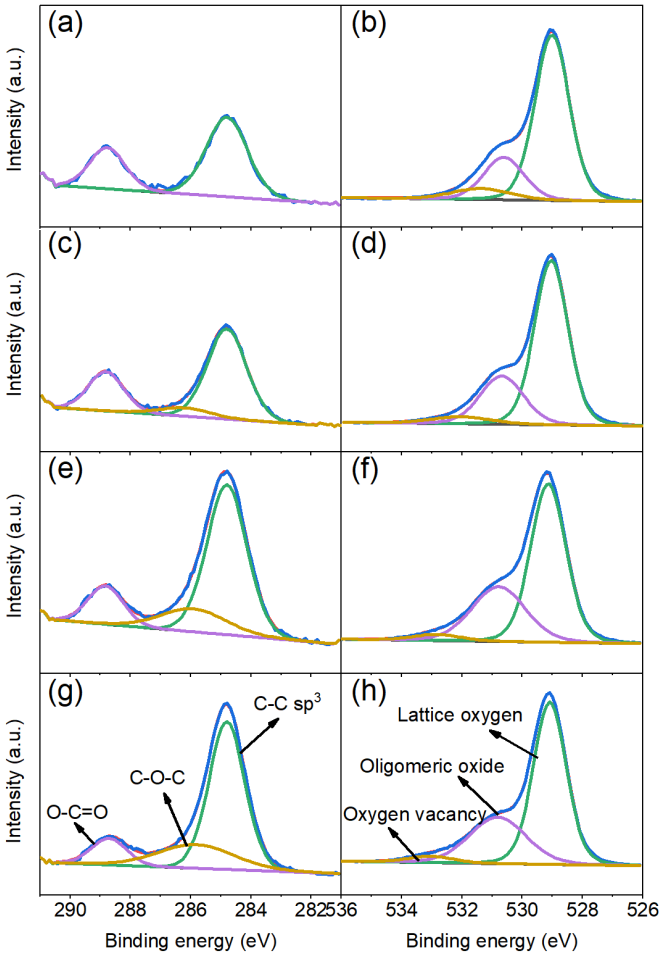

Figure S7. Deconvolutions of XPS spectra: C1s and O1s spectra of K-0.82-FeIn/Ce-ZrO_2 (a and b), K-0.82-FeIn/Ce-ZrO_2_500 (c and d), K-0.82-FeIn/Ce-ZrO_2_700 (e and f) and K-0.82-FeIn/Ce-ZrO_2_900 (g and h).

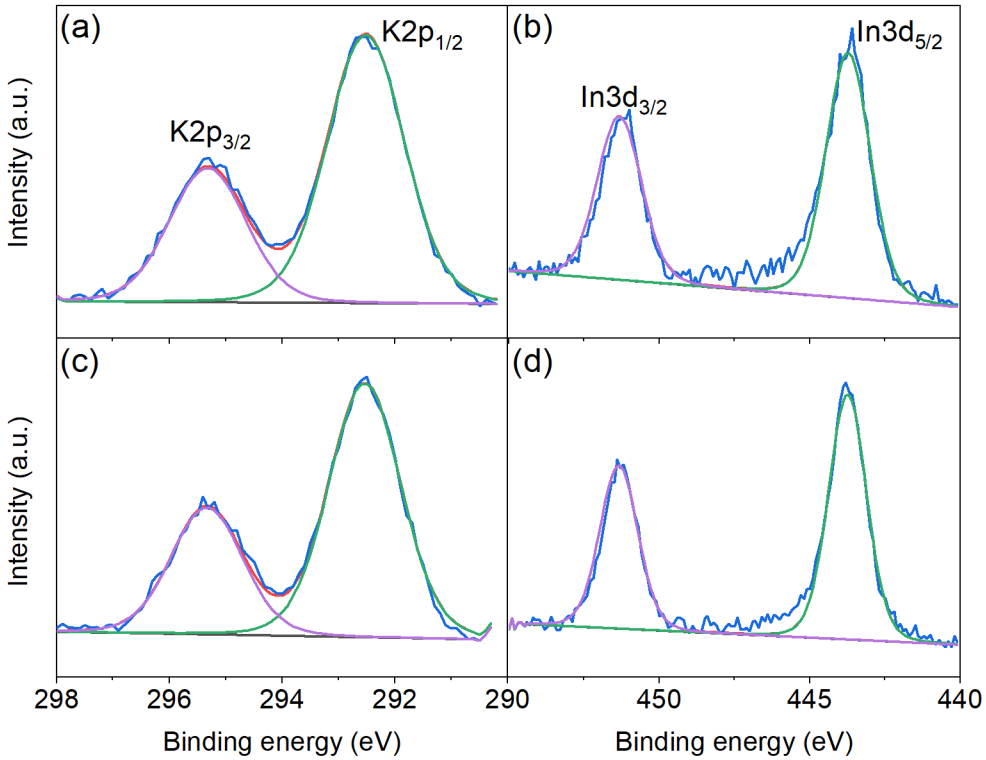

Figure S8. Deconvolutions of XPS spectra: K2p and In3d spectra of K-0.82-FeIn/Ce-ZrO_2_900 (a and b) and K-0.82-FeIn/Ce-ZrO_2_900 after a CO treatment (c and d).

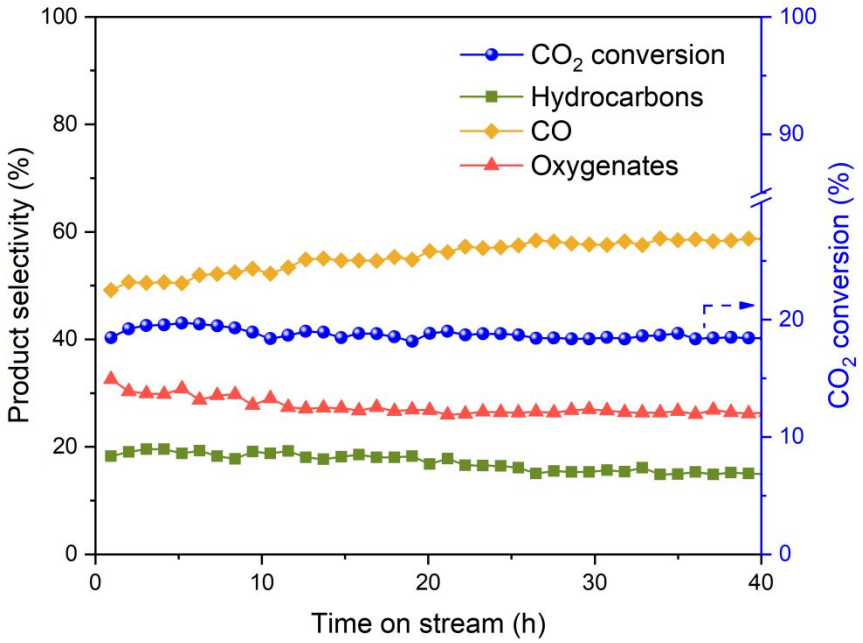

Figure S9. Representative graph for CO conversion and product selectivity versus time on stream for the K-0.48-FeIn/Ce-ZrO_2 catalyst after CO treatment. Reaction conditions: 300 °C, 10 MPa, GHSV = 4500 mL g^{-1} h^{-1}, H_2/CO_2 = 3.

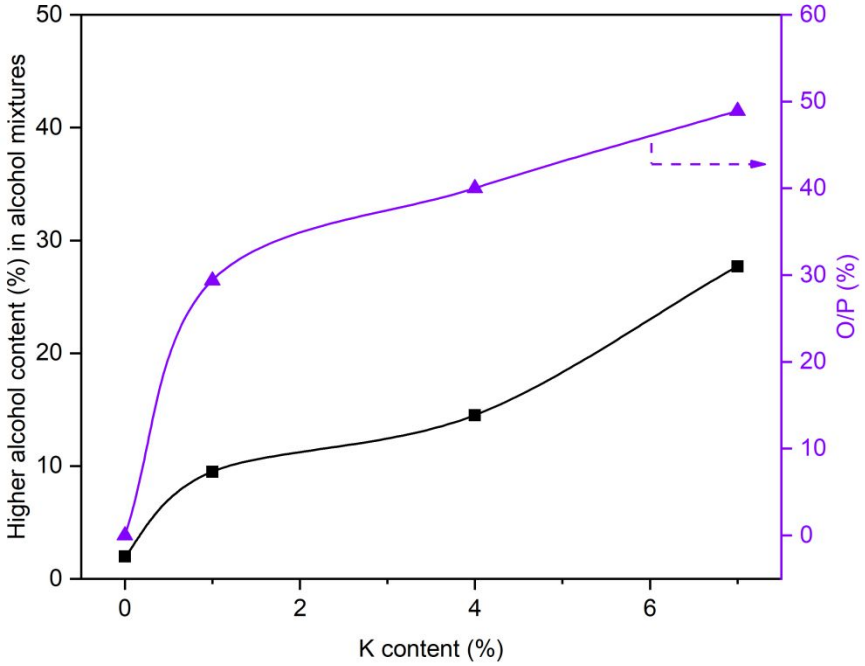

Figure S10. HA content in alcohol mixtures and the olefinic selectivity (O/P) for 0.48-FeIn/Ce-ZrO_2 catalysts with different K contents after CO treatment. Reaction conditions: 300 °C, 10 MPa, GHSV = 4500 mL g^{-1} h^{-1}, H_2/CO_2 = 3.

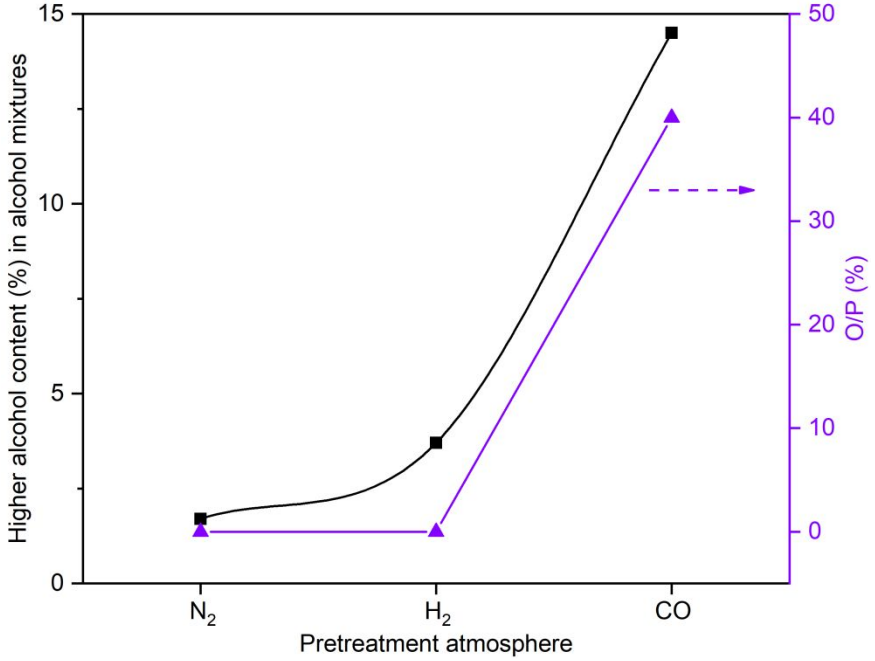

Figure S11. HA content in alcohol mixtures and the olefinic selectivity (O/P) for K-0.48-FeIn/Ce-ZrO_2 catalysts (4% K) after pretreated under different atmospheres. Reaction conditions: 300 °C, 10 MPa, GHSV = 4500 mL g^{-1} h^{-1}, H_2/CO_2 = 3.

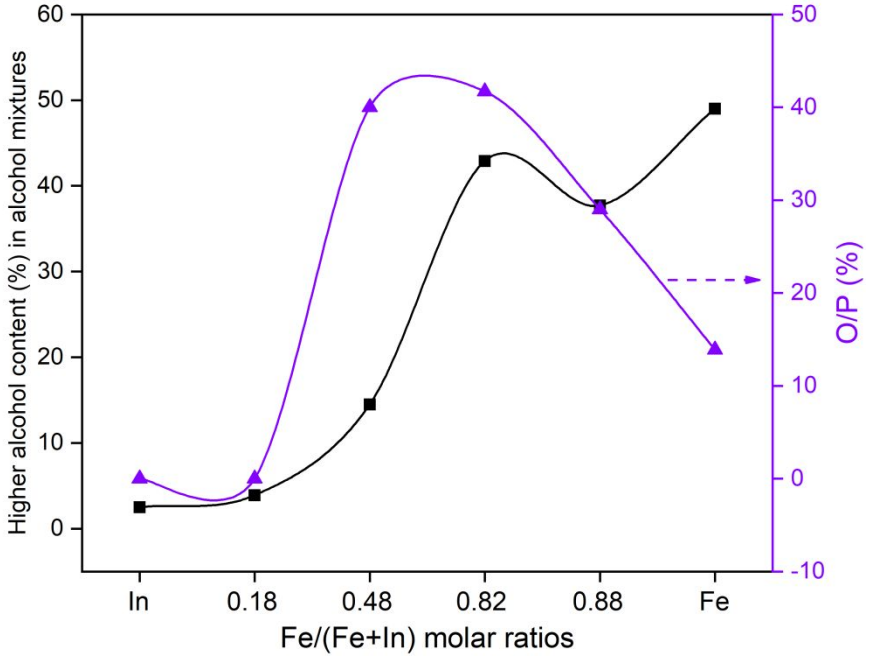

Figure S12. HA content in alcohol mixtures and the olefinic selectivity (O/P) for K-In/Ce-ZrO_2, K-Fe/Ce-ZrO_2 and K-FeIn/Ce-ZrO_2 catalysts with different Fe/(Fe+In) molar ratios. Reaction conditions: 300 °C, 10 MPa, GHSV = 4500 mL g^{-1} h^{-1}, H_2/CO_2 = 3.

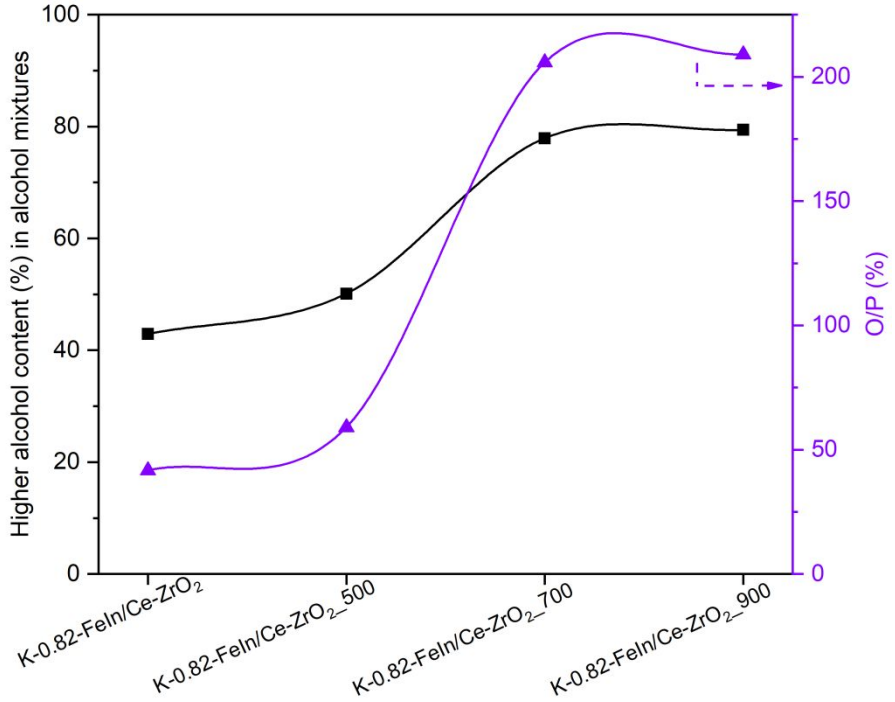

Figure S13. HA content in alcohol mixtures and the olefinic selectivity (O/P) for the uncalcined and calcined K-0.82-FeIn/Ce-ZrO_2 catalysts at different calcination temperatures. Reaction conditions: 300 °C, 10 MPa, GHSV=4500 mL g^{-1} h^{-1}, H_2/CO_2 =3.

Table S4. Carbon chain growth probability of alcohols obtained over the uncalcined and calcined K-0.82-FeIn/Ce-ZrO_2 catalysts. Reaction conditions: 300 °C, 10 MPa, GHSV=4500 mL g^{-1} h^{-1}, H_2/CO_2=3.

Catalyst	Carbon chain growth probability
K-0.82-FeIn/Ce-ZrO_2	0.18[a]
K-0.82-FeIn/Ce-ZrO_2_500	0.27[a]
K-0.82-FeIn/Ce-ZrO_2_700	0.24[b]
K-0.82-FeIn/Ce-ZrO_2_900	0.26[b]

[a] Carbon chain growth probability of C1-C6 alcohols; [b] Carbon chain growth probability of C2-C6 alcohols

Table S5. Catalytic performance of the Fe/Ce-ZrO_2, In/Ce-ZrO_2, 0.48-FeIn/Ce-ZrO_2 and K-Ce-ZrO_2 (blank) catalyst (diluted with SiC) for CO_2 hydrogenation reaction. [a]

Catalyst & pretreatment atmosphere	X_{CO_2}[c] (%)	Selectivity (%)						Alcohols distribution (%)	
		CO	CH_4	C_{2-4} olefins[d]	C_{2-4} paraffins[e]	Others[f]	Alcohols	Methanol	HA
In/Ce-ZrO_2, N_2	16.2	28.6	1.3	0	0	0	70.1	97.2	2.8
[b]FeIn/Ce-ZrO_2, N_2	11.6	42.0	1.1	0	0	0	56.9	99.0	1.0
In/Ce-ZrO_2, CO	15.3	23.3	2.2	0	0	0	74.5	99.6	0.4
Fe/Ce-ZrO_2, CO	18.1	14.5	52.4	0	22.1	0.2	10.8	85.4	14.6
K-Ce-ZrO_2, CO	1.0	90.4	9.6	0	0	0	0	0	0

[a] Reaction conditions: 300 °C, 10 MPa, GHSV = 4500 mL g^{-1} h^{-1}, H_2/CO_2 = 3; [b] Fe/(Fe+In) molar ratio = 0.48; [c] CO_2 conversion; [d] Olefins with carbon number of 2 to 4; [e] Paraffins with carbon number of 2 to 4; [f] Other hydrocarbons and liquid oxygenates except alcohols.

Table S6. Catalytic performance of the un-calcined and calcined K-0.82-FeIn/Ce-ZrO_2 catalysts for CO_2 hydrogenation reaction. [a]

Catalyst	X_{CO_2}[d] (%)	Selectivity (%)						
		CH_4	C_{2-4} olefins[e]	C_{2-4} paraffins[f]	CO	Methanol	HA	Others[g]
K-0.82-FeIn/Ce-ZrO_2_900[b]	29.6	20.1	20.3	12.5	13.4	4.7	28.7	0.3
K-0.82-FeIn/Ce-ZrO_2_900[c]	29.3	18.9	20.6	12.2	15.5	4.2	28.2	0.4
SiC_900	10.8	59.4	3.6	16.0	16.8	3.1	1.0	0.1

[a] Reaction conditions: 300 °C, 10 MPa, GHSV = 4500 mL g^{-1} h^{-1}, H_2/CO_2 = 3; [b] Mixing K-0.82-FeIn/Ce-ZrO_2 catalyst and SiC before calcination; [c] Mixing K-0.82-FeIn/Ce-ZrO_2 catalyst and SiC after separate calcination; [d] CO_2 conversion; [e] Olefins with carbon number of 2 to 4; [f] Paraffins with carbon number of 2 to 4; [g] Other hydrocarbons and liquid oxygenates except alcohols.

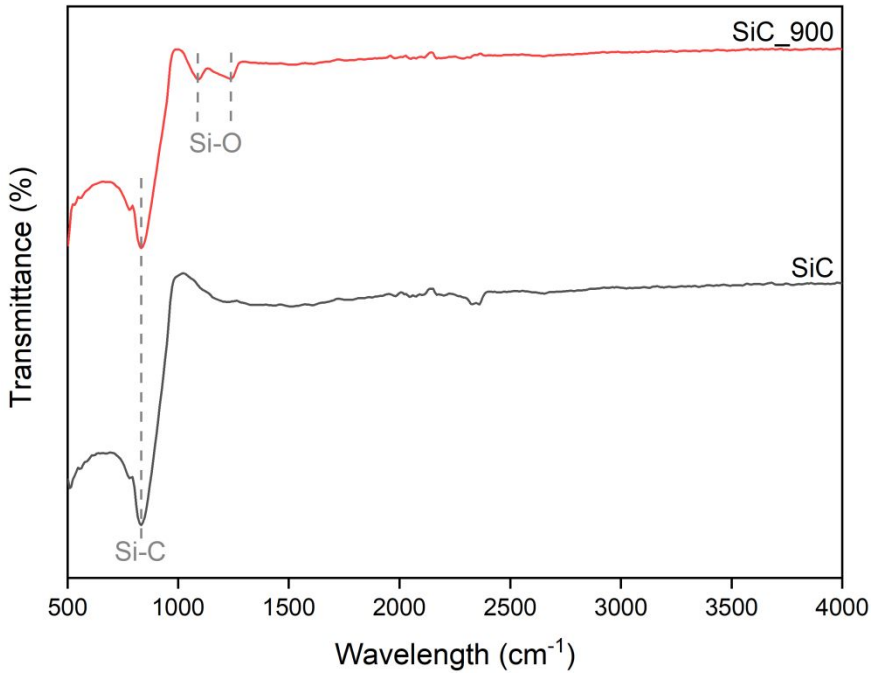

Figure S14. FTIR spectra of SiC before and after calcination in air at 900 °C.

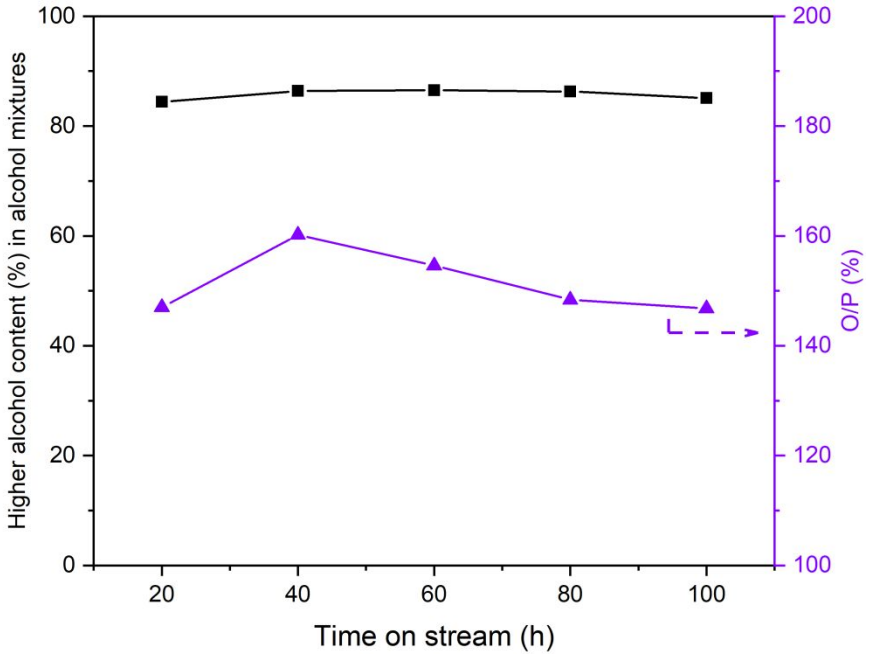

Figure S15. HA content in alcohol mixtures and the olefinic selectivity (O/P) versus runtime for the K-0.82-FeIn/Ce-ZrO_2 catalyst after calcination at 900 °C with the presence of SiC. Reaction conditions: 300 °C, 10 MPa, GHSV = 4500 mL g^{-1} h^{-1}, H_2/CO_2 = 3.

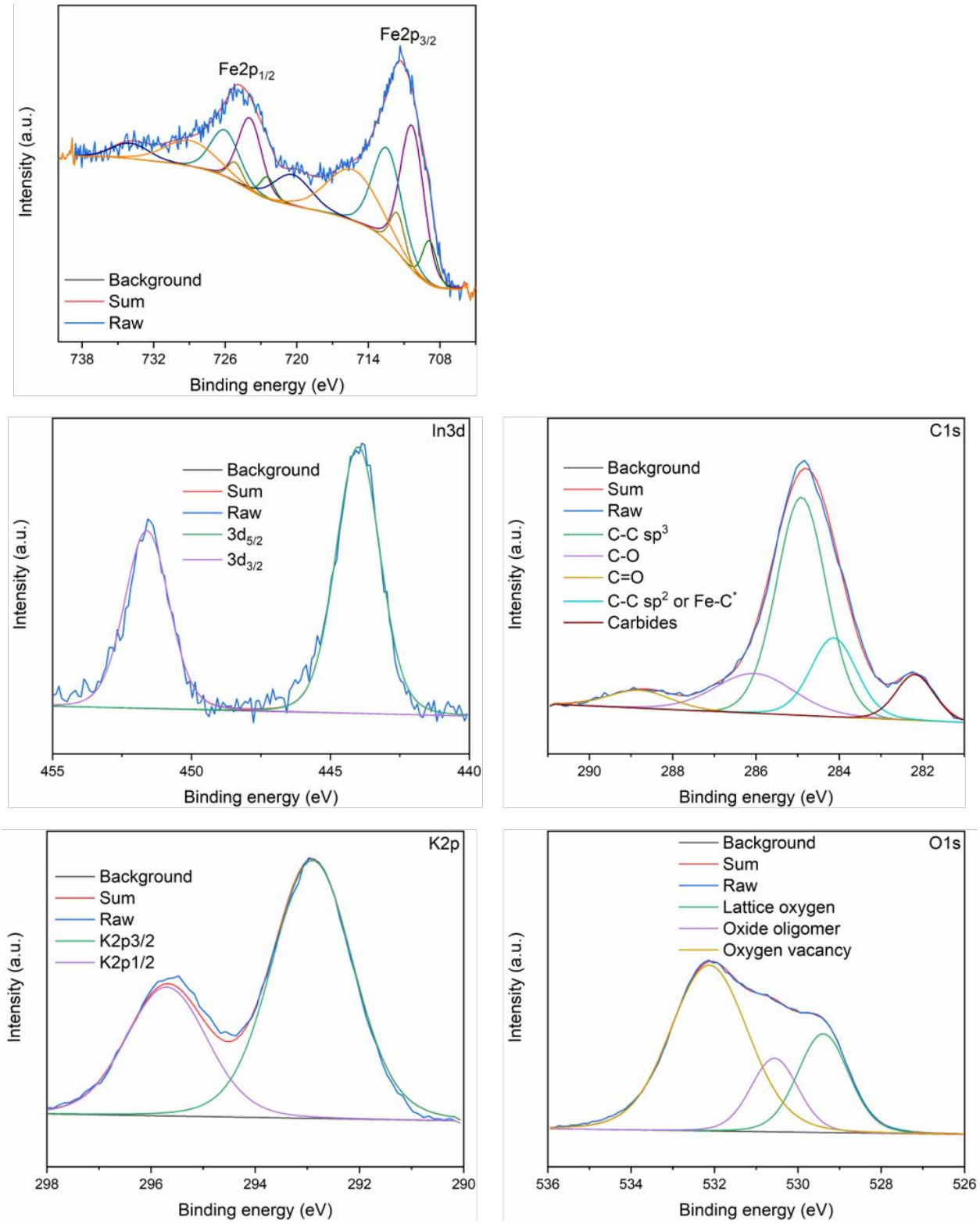

Figure S16. XPS spectra (Fe2p, In3d, K2p, C1s and O1s) of K-0.82-FeIn/Ce-ZrO_2_900 after reaction.

Table S7. Relative ratio's (%) of the C1s, O1s and Fe2p peak area for fresh K-0.82-FeIn/Ce-ZrO_2_900 after CO treatment and spent catalyst.

Items		K-0.82-FeIn/Ce-ZrO_2_900 after CO treatment	Spent catalyst
C1s	C-C sp^3	65.09	52.72
	C-O-C	19.66	15.58
	O-C=O	11.46	5.38
	C-C sp^2 or Fe-C*	3.79	17.86
	Carbides		8.46
O1s	Lattice oxygen	54.81	23.57
	Oligomeric oxide	29.46	16.28
	Oxygen vacancy	15.73	60.14
Fe2p	Fe^{3+}	50.30	39.81
	Fe^{2+}	39.75	54.51
	Fe-C	9.95	5.70

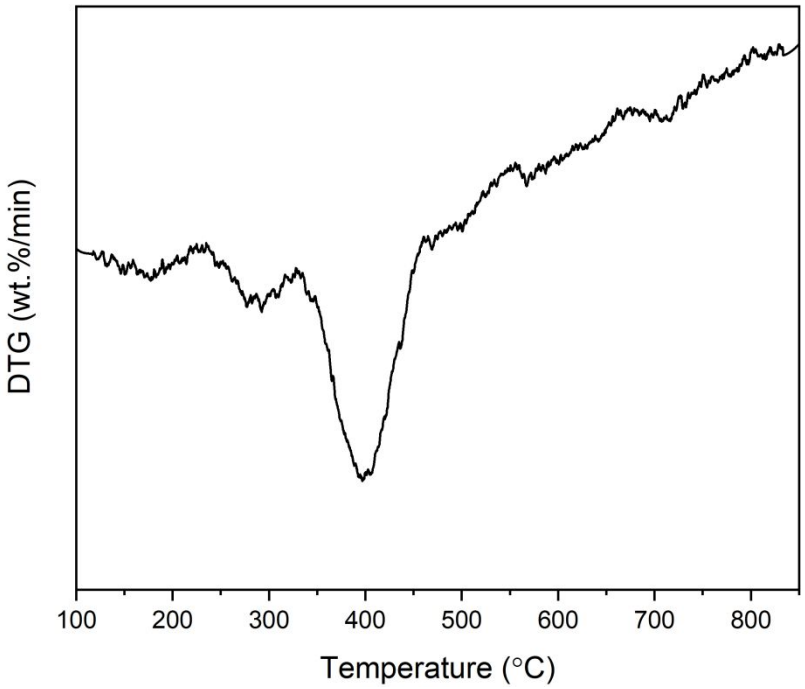

Figure S17. DTG curve of the K-0.82-FeIn/Ce-ZrO_2_900 (with SiC) catalyst after reaction.

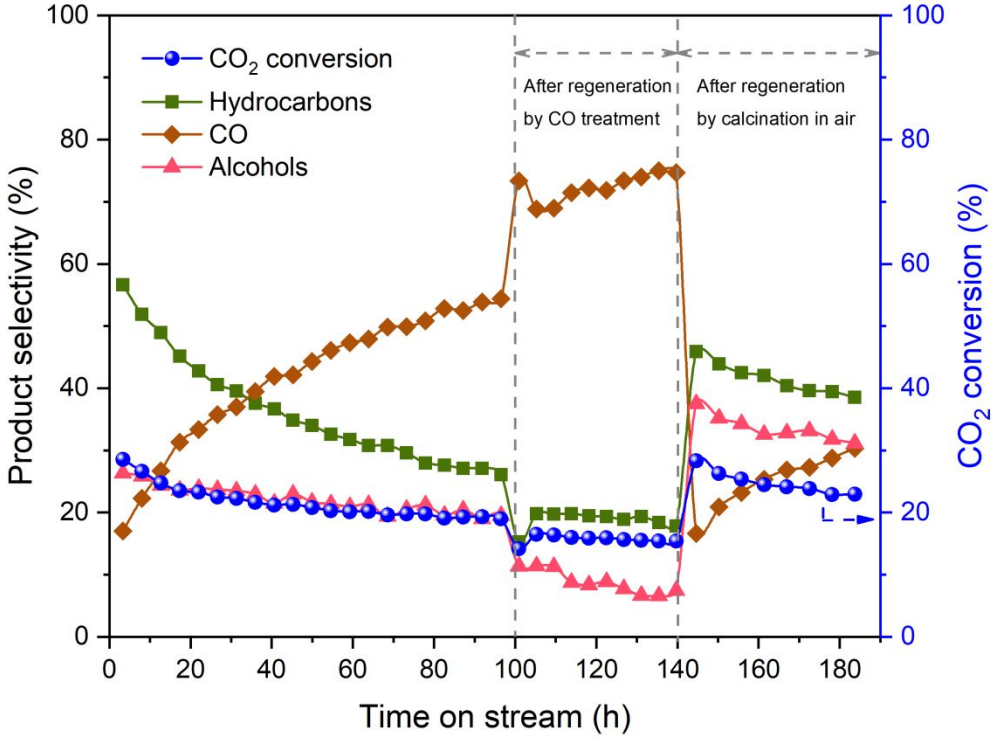

Figure S18. CO_2 conversion and product selectivity versus runtime for the K-0.82-FeIn/Ce-ZrO_2 catalyst. Reaction conditions: 300 °C, 10 MPa, GHSV=4500 mL g^{-1} h^{-1}, H_2/CO_2 =3.

Table S8. Literature benchmarks of HA synthesis from CO_2 hydrogenation (H_2/CO_2 = 3) over varied catalysts.

Entry	Catalyst	T[a] (°C)	P[b] (MPa)	GHSV[c] (cm^3 g_{cat}^{-1} h^{-1})	X_{CO_2}[d] (%)	S_{CO}[e] (%)	S_{HC}[f] (%)	S_{MeOH}[g] (%)	S_{HA}[h] (%)	Y_{HA}[i] (%)	Ref.
1	KFeIn/Ce-ZrO_2	300	10	4500	29.6	13.4	53.2	4.7	28.7	8.5	This work
2	KCuZnFe	300	6	5000[j]	42.3	6.9	56.4	4.7	31.9	13.5	[7]
3	Pd-KGaFeZn-KCuZnAl	330	8.1	20000[j]	54.5	9.7	64.5	5.2	17.0	9.3	[8]
4	Co/LaGaO	240	3	3000	9.8	0	25.3	12.1	62.6	6.1	[9]
5	LiRhFe/TiO_2	250	3.04	6000	15.7	12.5	53.9	2.2	31.3	4.9	[10]
6	RhFe/SiO_2	260	5	6000[j]	26.7	19.7	34.7	29.2	16.0	4.3	[11]
7	KCuZnFe/ZrO_2	320	3	3600[j]	25.5	53.1	23.6	14.3	11.4	2.9	[12]
8	Co_3O_4	200	2	6000	28.9	0	~80.8	10.2	9.0	2.6	[13]
9	NaCo/SiO_2	250	5	4000[j]	10.7	28.3	~24.5	23.6	23.6	2.5	[14]
10	KCuZn/KCuFeCo	350	6	5000[j]	32.4	45.3	~42.9	5.3	6.5	2.1	[15]
11	CoMoS	340	10.4	0.43[k]	32.0	57.5	16.5	20.0	6.0	1.9	[16]
12	LiRhMn/SiO_2	240	5	6000	16.1	2.4	88.6	1.3	7.7	1.2	[17]
13	Pt/Co_3O_4	200	2	6000	27.3	0	80.1	15.7	4.2	1.1	[18]

[a] Reaction temperature; [b] Reaction pressure; [c] Gas hourly space velocity; [d] CO_2 conversion; [e] CO selectivity; [f] Hydrocarbons selectivity; [g] Methanol selectivity; [h] HA selectivity; [i] HA yield; [j] h^{-1}; [k] g g_{cat}^{-1} h^{-1}

REFERENCES

1. Mears, D. E., Tests for transport limitations in experimental catalytic reactors. *Industrial & Engineering Chemistry Process Design and Development* **1971,** *10* (4), 541-547, DOI: 10.1021/i260040a020
2. Chandra, V.; Peters, E.A.J.F.; Kuipers, J.A.M., Direct numerical simulation of a non-isothermal non-adiabatic packed bed reactor. *Chemical Engineering Journal* **2020**, 385, 123641, DOI: 10.1016/j.cej.2019.123641
3. Slattery, J. C.; Bird, R. B., Calculation of the diffusion coefficient of dilute gases and of the self-diffusion coefficient of dense gases. *AIChE Journal* **1958,** *4* (2), 137-142, DOI: 10.1002/aic.690040205
4. Bird, R. B.; Stewart, W. E.; Lightfoot, E. N., Transport Phenomena, Revised 2nd Edition. John Wiley & Sons, Inc: **2009**, DOI: https://www.wiley.com/en-us/Transport+Phenomena%2C+Revised+2nd+Edition-p-9780470508633
5. Weisz, P. B.; Prater, C. D., Interpretation of measurements in experimental catalysis. *Adv. Catal* **1954,** *6* (143), 60390-9, DOI: 10.1016/S0360-0564(08)60390-9
6. Satterfield, C. N., Citation classic-mass-transfer in heterogeneous catalysis. *CURRENT CONTENTS/ENGINEERING TECHNOLOGY & APPLIED SCIENCES* **1979,** (41), E10-E10, DOI: http://garfield.library.upenn.edu/classics1979/A1979HM63100001.pdf
7. Li, S.; Guo, H.; Luo, C.; Zhang, H.; Xiong, L.; Chen, X.; Ma, L., Effect of iron promoter on structure and performance of K/Cu–Zn catalyst for higher alcohols synthesis from CO_2 hydrogenation. *Catalysis letters* **2013,** *143* (4), 345-355, DOI: 10.1007/s10562-013-0977-7
8. Yamamoto, T.; Inui, T., Highly effective synthesis of ethanol from CO_2 on Fe, Cu-based novel catalysts. *Studies in Surface Science and Catalysis*, Elsevier: **1998**; Vol. 114, pp 513-516, DOI: 10.1016/S0167-2991(98)80809-4
9. Zheng, J.-n.; Kang, A. N.; Wang, J.-m.; Jing, L. I.; Yuan, L. I. U., Direct synthesis of ethanol via CO_2 hydrogenation over the Co/La-Ga-O composite oxide catalyst. *Journal of Fuel Chemistry and Technology* **2019,** *47* (6), 697-708, DOI: 10.1016/S1872-5813(19)30031-3
10. Yang, C.; Mu, R.; Wang, G.; Song, J.; Tian, H.; Zhao, Z.-J.; Gong, J., Hydroxyl-mediated ethanol selectivity of CO_2 hydrogenation. *Chemical science* **2019,** *10* (11), 3161-3167, DOI: 10.1039/C8SC05608K
11. Kusama, H.; Okabe, K.; Sayama, K.; Arakawa, H., Ethanol synthesis by catalytic hydrogenation of CO_2 over Rh/$FeSiO_2$ catalysts. *Energy* **1997,** *22* (2-3), 343-348, DOI: 10.1016/S0360-5442(96)00095-3
12. Guo, W.; Gao, W. G.; Wang, H.; Tian, J. J. In *Higher Alcohols Synthesis from CO_2 Hydrogenation over K_2O-Modified $CuZnFeZrO_2$ Catalysts* **2014**; Trans Tech Publ: pp 20-24, DOI: 10.4028/www.scientific.net/AMR.827.20
13. Liu, B.; Ouyang, B.; Zhang, Y.; Lv, K.; Li, Q.; Ding, Y.; Li, J., Effects of mesoporous structure and Pt promoter on the activity of Co-based catalysts in low-temperature CO_2 hydrogenation for higher alcohol synthesis. *Journal of Catalysis* **2018,** *366*, 91-97, DOI: 10.1016/j.jcat.2018.07.019
14. Zhang, S.; Liu, X.; Shao, Z.; Wang, H.; Sun, Y., Direct CO_2 hydrogenation to ethanol over supported Co2C catalysts: Studies on support effects and mechanism. *Journal of Catalysis* **2020,** *382*, 86-96, DOI: 10.1016/j.jcat.2019.11.038
15. Guo, H.; Li, S.; Peng, F.; Zhang, H.; Xiong, L.; Huang, C.; Wang, C.; Chen, X., Roles Investigation of Promoters in K/Cu–Zn Catalyst and Higher Alcohols Synthesis from CO_2 Hydrogenation over a Novel Two-Stage Bed Catalyst Combination System. *Catalysis Letters* **2015,** *145* (2), 620-630, DOI: 10.1007/s10562-014-1446-7
16. Nieskens, D. L. S.; Ferrari, D.; Liu, Y.; Kolonko Jr, R., The conversion of carbon dioxide and hydrogen into methanol and higher alcohols. *Catalysis Communications* **2011,** *14* (1), 111-113, DOI: 10.1016/j.catcom.2011.07.020

17. Kusama, H.; Okabe, K.; Sayama, K.; Arakawa, H., CO_2 hydrogenation to ethanol over promoted Rh/SiO2 catalysts. *Catalysis today* **1996,** *28* (3), 261-266, DOI: 10.1016/0920-5861(95)00246-4
18. Ouyang, B.; Xiong, S.; Zhang, Y.; Liu, B.; Li, J., The study of morphology effect of Pt/Co3O4 catalysts for higher alcohol synthesis from CO_2 hydrogenation. *Applied Catalysis A: General* **2017,** *543*, 189-195, DOI: 10.1016/j.apcata.2017.06.031